

Helicity-Flux-Driven Alpha Effect in Laboratory and Astrophysical Plasmas

F. Ebrahimi¹ and A. Bhattacharjee^{1,2}

¹*Center for Magnetic Self-Organization, Department of Astrophysical Sciences, Princeton University, Princeton, NJ 08544*

²*Princeton Plasma Physics Laboratory, Princeton, NJ 08543*

(Dated: December 3, 2024)

The constraint imposed by magnetic helicity conservation on the alpha effect is considered for both magnetically and flow dominated self-organizing plasmas. Direct numerical simulations are presented for a dominant contribution to the alpha effect, which can be cast in the functional form of a total divergence of an averaged helicity flux, called the helicity-flux-driven alpha ($H\alpha$) effect. Direct numerical simulations of the $H\alpha$ effect are presented for two examples—the magnetically dominated toroidal plasma unstable to tearing modes, and the flow-dominated accretion disk.

Large-scale magnetic fields have been observed in widely different types of astrophysical objects, such as planets and stars, as well as accretion disks and galaxies. The source of this magnetic field is the well-known dynamo effect, which has stimulated an extensive search for models in which large-scale magnetic fields are self-generated from turbulence and sustained despite the presence of dissipation. The point of departure of most theoretical and computational studies of this problem is magnetohydrodynamics (MHD), represented by intrinsically nonlinear equations that describe the self-consistent evolution of a magnetized fluid. A standard approach to the problem is mean-field theory, in which a fluctuation-induced electromotive force (emf) parallel to the mean magnetic field is obtained from the vector product of flow and magnetic field fluctuations. This is known as the alpha effect, which holds a key to how large-scale magnetic fields may grow out of turbulence, beginning from a seed field.

While kinematic dynamo theory [1] predicts the existence of the alpha effect in astrophysical settings given a complex velocity field, its magnitude and saturation in a fully nonlinear, self-consistent theory has been a subject of significant controversy. Since this problem appears to be just as difficult as the problem of MHD turbulence, one constructive approach is to examine the constraints imposed by rigorous conservation laws of MHD on the functional form of the alpha effect. In this context, the role of magnetic helicity, which is a “rugged invariant” of MHD turbulence [2], has received significant attention. [3]

In this Letter, we revisit the role of magnetic helicity flux on the alpha effect. We do so by considering two completely different physical examples from a common perspective. The first example is a magnetically dominated self-organized toroidal plasma such as the reversed field pinch (RFP) in which the alpha effect is instrumental in converting one type of magnetic flux into another by the intervention of tearing instabilities while the total magnetic energy decays. The second example is a flow-driven accretion disk, which too exhibits self-organization, and where there is compelling evidence

from several MHD simulations that a large-scale magnetic field is produced and sustained by the nonlinear evolution of the magnetorotational instability (MRI). [4] The fluctuation-induced alpha effect due to the MRI results in the generation of large-scale magnetic field, which can cause MRI saturation [5]. We demonstrate by analysis and direct numerical simulations (DNS) that in both cases a dominant contribution to the alpha effect can be cast in the functional form of a total divergence of an averaged helicity flux, which we call the helicity-flux-driven alpha effect (hereafter simply referred to as the $H\alpha$ effect), and is represented by the last term in Eq. 3 below. In the case of the RFP, the $H\alpha$ effect reduces to “hyper-resistivity” [6–8], often invoked by the MHD turbulence community but demonstrated here to emerge from DNS of tearing modes. In the case of the accretion disk, the $H\alpha$ effect leads to a new type of flux that is related to, but is more complete than, the so-called Vishniac-Cho flux [9], which was obtained by a heuristic reduction of the nonlinear MHD equations, and has been invoked in recent astrophysical dynamo studies. [10, 11] Here, we demonstrate from a global MRI simulation [5] that the $H\alpha$ effect plays a critical role in the self-generation of the large-scale magnetic field. Viewed together, these two different physical applications reinforce the importance of the constraint Eq. 3, derived rigorously from the MHD equations, and the $H\alpha$ effect that emerges from it.

We begin with a discussion of the constraint equation, which was first discussed in [6] in the context of the RFP, and later in a form more relevant for astrophysical applications in [12] as well as [13]. Using the equations for the time-derivative of the vector potential \mathbf{B} and magnetic field \mathbf{A} , given by Maxwells equations $\partial\mathbf{A}/\partial t = -\mathbf{E} - \nabla\phi$ and $\partial\mathbf{B}/\partial t = -\nabla \times \mathbf{E}$, where ϕ is the electrostatic potential, we obtain

$$\frac{1}{2} \frac{\partial(\mathbf{A} \cdot \mathbf{B})}{\partial t} + \frac{1}{2} \nabla \cdot \Gamma_k = -\mathbf{E} \cdot \mathbf{B}. \quad (1)$$

where $\Gamma_k = (-\mathbf{A} \times \mathbf{E} + \mathbf{A} \times \nabla\phi) = -2\mathbf{A} \times \mathbf{E} - \mathbf{A} \times \partial\mathbf{A}/\partial t$ is defined as the total magnetic helicity flux. All variables are decomposed as $f = \langle f \rangle + \tilde{f}$, where $\langle f \rangle = \bar{f}$ is the *mean* component (where $\langle \dots \rangle$ denotes the azimuthal and axial average), and \tilde{f} is the fluctuating component.

It can be shown that, [12, 13]

$$\frac{1}{2} \frac{\partial \langle \tilde{\mathbf{A}} \cdot \tilde{\mathbf{B}} \rangle}{\partial t} + \frac{1}{2} \nabla \cdot \langle \Gamma_k \rangle = - \langle \tilde{\mathbf{E}} \cdot \tilde{\mathbf{B}} \rangle. \quad (2)$$

We now use the perturbed form of Ohms law for a resistive MHD plasma, $\tilde{\mathbf{E}} = -\tilde{\mathbf{V}} \times \tilde{\mathbf{B}} - \tilde{\mathbf{V}} \times \tilde{\mathbf{B}} + \eta \tilde{\mathbf{J}}$, which implies that $\varepsilon_{emf} \cdot \tilde{\mathbf{B}} = \langle \tilde{\mathbf{V}} \times \tilde{\mathbf{B}} \cdot \tilde{\mathbf{B}} \rangle = -\eta \langle \tilde{\mathbf{J}} \cdot \tilde{\mathbf{B}} \rangle + \langle \tilde{\mathbf{E}} \cdot \tilde{\mathbf{B}} \rangle$, which when combined with Eq. 2, yields the exact result

$$\varepsilon_{emf} \cdot \tilde{\mathbf{B}} = -\eta \langle \tilde{\mathbf{J}} \cdot \tilde{\mathbf{B}} \rangle - \frac{1}{2} \frac{\partial}{\partial t} \langle \tilde{\mathbf{A}} \cdot \tilde{\mathbf{B}} \rangle + H\alpha \quad (3)$$

where

$$H\alpha = -\frac{1}{2} \nabla \cdot \langle \Gamma_k \rangle = \nabla \cdot [\langle \tilde{\mathbf{A}} \times \tilde{\mathbf{E}} \rangle + \frac{1}{2} \langle \tilde{\mathbf{A}} \times \frac{\partial \tilde{\mathbf{A}}}{\partial t} \rangle]. \quad (4)$$

Equations 3 and 4 are completely general, and serve as the point of departure for both of our examples, discussed below. Specifically, for both examples, the $H\alpha$ effect will be calculated using Eq. 4. We employ the nonlinear, resistive MHD code, DEBS, which solves the single fluid MHD equations in doubly periodic (r, ϕ, z) cylindrical geometry [5, 14]. We use the same normalization as in [5, 14], where time, radius and velocity are normalized to the outer radius a , the resistive diffusion time $\tau_R = a^2/\mu_0\eta$, and the Alfvén velocity $V_A = B_0/\sqrt{\mu_0\rho_0}$, respectively (B_0 and ρ_0 are the values on axis). The dimensionless parameters, $S = \tau_R V_A/a$ and P_m , are the Lundquist number and the magnetic Prandtl number (the ratio of viscosity to resistivity), respectively. For magnetically dominated simulations a force-free initial condition is used [15]. For the flow dominated MRI simulations, the initial state satisfies the equilibrium force balance condition $\frac{\beta_0}{2} \nabla p = \rho V_\phi^2/r$, where $\beta_0 = 2\mu_0 P_0/B_0^2$ is the beta normalized to the axis value, and the initial pressure and density profiles are assumed to be radially uniform and nonstratified. Pressure and density are evolved; however, they remain fairly uniform during the computations. In these computations, a mean Keplerian profile ($V_\phi \propto r^{-1/2}$) is maintained in time by an external ad-hoc force in the momentum equation. The boundary conditions in the radial direction are as are appropriate for dissipative MHD with a perfectly conducting boundary: the tangential electric field, the normal component of the magnetic field, and the normal component of the velocity vanish, and the tangential component of the velocity is the rotational velocity of the wall. The azimuthal (ϕ) and axial (z) directions are periodic. The boundary conditions on the vector potential keep the volume-integrated magnetic helicity gauge-invariant.

In magnetically dominated laboratory configurations like the RFP, the importance of magnetic helicity is well recognized due to the efficiency of the Taylor relaxation process [16]. In these configurations, it has been experimentally demonstrated that a turbulent plasma relaxes

to a state of minimum energy subject to the conservation of total magnetic helicity [17, 18]. There is strong evidence from experiments as well as simulations [15] that tearing instabilities resonant with rational surfaces within the plasma play an important role in the relaxation process. The tearing fluctuations contribute to the emf ε_{emf} , which converts toroidal flux to poloidal flux.

To calculate ε_{emf} due to tearing instabilities, we consider a general cylindrical equilibrium magnetic field $\mathbf{B} = B_z(r)\hat{z} + B_\phi(r)\hat{\phi}$ which is subject to perturbations of the form $\tilde{f}(r, \phi, z, t) = \tilde{f}(r) \exp(\gamma t + im\phi - inz/R)$ in cylinder of radius a and periodicity length $2\pi R$ along z . In this geometry, reconnection driven by tearing instabilities tend to occur at mode-rational surfaces located at $r = r_s$, where $q = rB_z(r)/RB_\phi(r) = m/n$ and m and n are positive integers. At these resonant surfaces, the parallel wave number vector vanishes, that is $\mathbf{k} \cdot \mathbf{B} = mB_\phi/r - nB_z/R = 0$.

For reconnecting instabilities, we adopt tearing ordering [19, 20] $\gamma \propto \eta^{3/5}$, $\gamma \rightarrow \epsilon^3$, $\eta \rightarrow \epsilon^5$, $(r - r_s) \rightarrow \epsilon^2 x$, where ϵ is a small parameter. Using this ordering, it can be shown that to leading order, one obtains

$$\varepsilon_{emf} \cdot \tilde{\mathbf{B}} = \nabla \cdot (\kappa^2 \nabla \frac{\mathbf{J} \cdot \tilde{\mathbf{B}}}{B^2}) \quad (5)$$

where κ^2 is a positive-definite functional [6–8]. Here, we further extend the derivation of κ^2 to obtain the radial extent and the structure of hyperresistivity around the reconnection surface in terms of Hermite polynomials to obtain,

$$\kappa^2 = \frac{B^2}{kr_s} \eta Q \Psi_0^2 \zeta(r), \quad (6)$$

$$\zeta(r) = \exp[-(Q^{-1/2}(r - r_s))^2/2] \sum_m a_{2m} H_{2m}[Q^{-1/4}(r - r_s)],$$

$$a_{2m} = \frac{2^{1/2}}{4^m m!} \left[\frac{1}{Q^{3/2}} (4m + 1) \right], \quad (7)$$

where Q and S_q are the normalized growth rate and shear factor, defined as $Q = \gamma/(l^4 Q_R)$ and $S_q = (\frac{2a}{Rq'})^2$, where prime indicates radial derivative ($Q_R = (\frac{m^2 \eta F'^2 B^2}{\rho r_s^2})^{1/3}$, $l = (L_R/r_s)^{1/5}$, $L_R = (\eta/Q_R)^{1/2}$, $F' = -\frac{q'B_\theta}{qB}$). We note that only the even parity solution for the perturbed radial displacement contributes to $H\alpha$ under the constant-psi approximation, represented by the constant Ψ_0 . (We adopt here the notation of [21].)

For a reconnecting tearing mode ($m=1$, $k=1.8$) resonant at $r=0.303$, with a mean parallel current, $\mathbf{J} \cdot \mathbf{B}/B^2 = 3.2(1 - r^3)$, the hyperresistivity, κ^2 , in the inner reconnection layer can directly be obtained analytically from Eqs. 6 and 7, which shows a radial extent of about 0.05 (here we have normalized r to the minor radius a). In

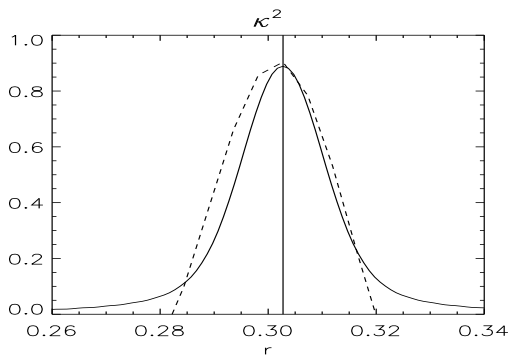


FIG. 1. The radial structure of hyperresistivity, κ^2 for a single tearing mode with $S = 10^6$. The solid line denotes the analytical result, while the dashed line shows the numerical result in the vicinity of the reconnecting surface where linear theory is applicable. The reconnecting surface is shown at $r = r_s$ with the vertical line.

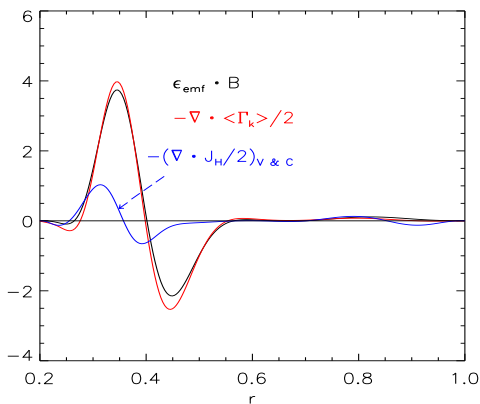


FIG. 2. Dynamo term $\varepsilon_{emf} \cdot \mathbf{B}$, total divergence form of fluctuation-induced helicity flux given in equation (5) $-\nabla \cdot \langle \Gamma_k \rangle / 2$, and the divergence form of helicity flux given by Vishniac & Cho, during $m=1$ MRI mode nonlinear saturation.

Fig. 1, we compare the analytical result with the numerical result obtained from a single tearing mode computation. Both results demonstrate the positivity of κ^2 , required by conservation laws. [6, 7] The dashed line represents the numerical result from the leading term in Eq. 3, and the solid line the analytical result. We should note that the computations are in the viscous-resistive regime with $S = 10^6$ and $Pm=1$, which results in a larger radial extent of κ^2 than the analytical result. We have also computed κ^2 from multiple nonlinear tearing modes, which shows a broadening from multiple modes. Thus, our DNS confirm for the first time the explicit functional form of Eq. 5. The predictions of Eq. 5 for the RFP are well-known—the mean-field saturated states in these magnetically dominated self-organized plasmas are Taylor-like [6–8], consistent with experimental observations [17, 18].

We now consider the $H\alpha$ effect in the context of the accretion disk, which is flow-driven and dominated by the MRI. In contrast to the magnetically dominated RFP,

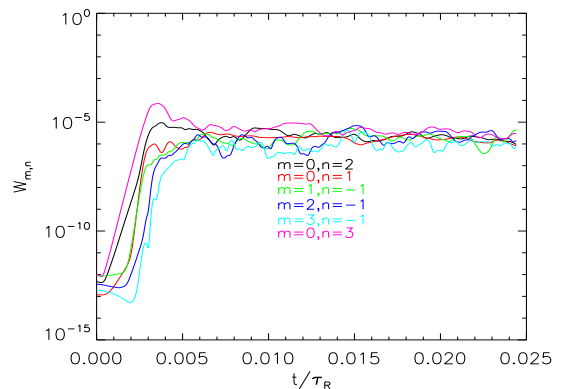


FIG. 3. Magnetic energy $W_{m,n} = 1/2 \int \tilde{B}_{r(m,n)}^2 dr^3$ vs time for different MRI modes for a fully nonlinear computations.

where the primary source of free energy is the parallel current density, the primary source of free energy in the accretion disk is the flow shear. Motivated in part by the considerations of [12], Vishniac and Cho [9] proposed a form of helicity-flux-driven flux of the form $(-\nabla \cdot J_H/2)_{VC}$ where $J_H = \langle (\tilde{\mathbf{E}} - \nabla \tilde{\phi}) \times \tilde{\mathbf{A}} \rangle = -2 \langle (\tilde{\mathbf{E}} \times \nabla \tilde{\phi}) \rangle > \tau_c$ where τ_c is the eddy correlation time. We demonstrate below by DNS that $(-\nabla \cdot J_H/2)_{VC}$ underestimates significantly the role of the $H\alpha$ effect. As is often standard practice in zero-net-flux MRI simulations, we begin with an initial magnetic field of the form $B_z = \sin(2\pi(r-r_1)/(r_2-r_1))/r$ and $B_\phi = 0$, driven by an azimuthal mean Keplerian flow ($V_\phi = V_0 r^{-1/2}$), where r_1 , r_2 and V_0 are the inner and outer radii and the magnitude of mean flow on axis, respectively. Figure 2 shows the result of a single non-axisymmetric $m=1$ mode computation of the MRI in which the various terms in Eq. 3 are calculated numerically for magnetic Reynolds number $Rm = SV_0/V_A = 1600$ (with $Pm = 1$), in a nonlinearly saturated state. It is seen that the term on the left-hand-side, given by $\varepsilon_{emf} \cdot \tilde{\mathbf{B}}$ is balanced almost entirely by $H\alpha$, and the contribution of the other two terms are small. For comparison, we also compute the Vishniac-Cho flux, which is much smaller than $H\alpha$. This is because the perturbed electric field computed in [9] is approximated by the relation $\tilde{\mathbf{E}} = -\tilde{\mathbf{V}} \times \tilde{\mathbf{B}}$, which is incomplete. Note that our computation of the $H\alpha$ effect begins with the exact Eq. 4, which differs from the approximate equations used in other studies [11, 22, 23] which have also identified additional contributions to the Vishniac-Cho flux.

We have also carried out DNS with multiple modes, leading to MRI turbulence. Full nonlinear computations start with a Keplerian flow profile and zero net-flux with $Pm = 2$, $Rm = 3400$, $\beta_0 = 10^5$, and radial, azimuthal and axial resolutions $n_r=220$, $0 < m < 43$ and $-43 < n < 43$, respectively. The radial magnetic energy for MRI modes is shown in Fig. 3. As shown, the axisymmetric $m=0$ modes as well as the non-axisymmetric modes ($m=1,2,3$ are shown) grow robustly in the linear regime and satu-

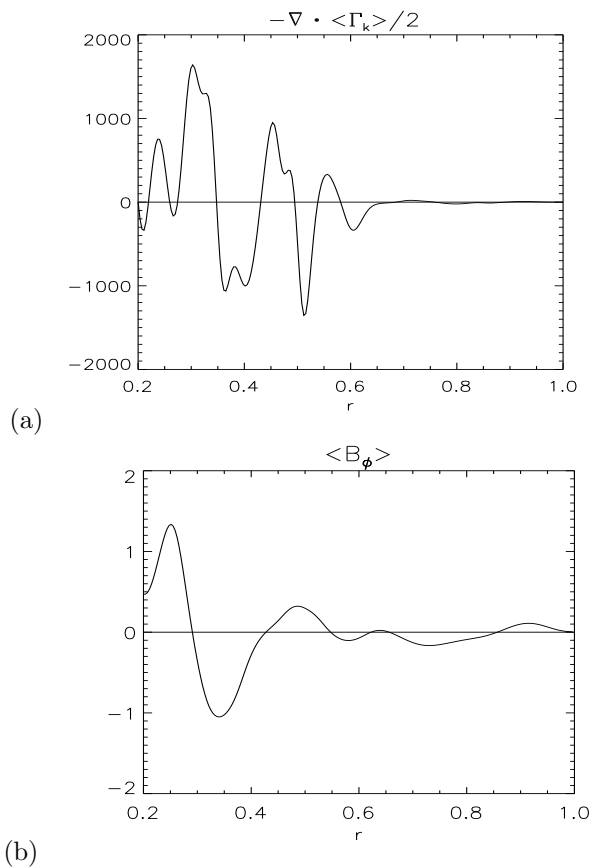


FIG. 4. The radial profiles of (a) $H\alpha$ for all the MRI modes (b) large-scale mean azimuthal magnetic field generated, averaged over three points in time ($t/\tau_R=0.6, 0.62, 0.65$).

rate non-linearly. The nonlinear saturated state exhibits significant time-dependence, including the second term on the right-hand-side of Eq. 3. In Fig. 4 (a), we show the time-averaged $H\alpha$ profile over three instants of time, and the averaged (along ϕ and z directions) B_ϕ profile. Since the initial state had no B_ϕ , it is clear that the $H\alpha$ effect plays a dominant role in producing a large-scale azimuthal field which, in turn, contributes to the nonlinear saturation of the MRI [5]. (The Vishniac-Cho flux continues to be much smaller than $H\alpha$ under these circumstances.)

In conclusion, we have demonstrated by DNS in global geometry that the $H\alpha$ effect, which is a rigorous consequence of magnetic helicity conservation in a turbulent plasma, plays a dominant role in magnetically as well as flow-driven self-organization. While the case of the magnetically dominated RFP, which has been the subject of numerous direct experimental observations, is relatively well understood, there remain many open questions in the case of the flow-driven MRI dynamo. Viewing both of these problems from a common perspective enables us to emphasize the importance of tracking the flow of magnetic helicity in quantitative measurements of the dynamo effect, which we have performed in this paper using

DNS beginning with the exact equations (3) and (4). It is also clear that the averaging process as well as the boundary conditions used can play a subtle role in such quantitative measurements. Such considerations might play an important role in resolving important differences in results between shearing box [24–26] and global MRI simulations.

This work was supported by the National Science Foundation grant No. 0962244 and by DOE, DE-FG02-12ER55142, DE-FG02-07ER46372, and CMSO. This work was also facilitated by the Max-Planck/Princeton Center for Plasma Physics. We thank J. Stone for several stimulating discussions and F. E. appreciates valuable discussions on the numerical techniques used in this paper with Dalton Schnack.

-
- [1] H. K. Moffatt, *Magnetic field generation in electrically conducting fluids* (1978).
 - [2] R. H. Kraichnan, *Physics of Fluids* **10**, 1417 (1967).
 - [3] See, for instance, the recent overview by E. G. Blackman, *Astronomische Nachrichten* **331**, 101 (2010), 0911.2315.
 - [4] S. A. Balbus and J. F. Hawley, *ApJ* **376**, 214 (1991).
 - [5] F. Ebrahimi, S. C. Prager, and D. D. Schnack, *Astrophys. J.* **698**, 233 (2009).
 - [6] A. Bhattacharjee and E. Hameiri, *Phys. Rev. Lett.* **57**, 206 (1986).
 - [7] A. H. Boozer, *J. Plasma Phys.* **35**, 133 (1986).
 - [8] H. R. Strauss, *Physics of Fluids* **29**, 3668 (1986).
 - [9] E. T. Vishniac and J. Cho, *ApJ* **550**, 752 (2001).
 - [10] S. Sur, A. Shukurov, and K. Subramanian, *MNRAS* **377**, 874 (2007), astro-ph/0612756.
 - [11] K. Subramanian and A. Brandenburg, *Physical Review Letters* **93**, 205001 (2004).
 - [12] A. Bhattacharjee and Y. Yuan, *ApJ* **449**, 739 (1995).
 - [13] E. G. Blackman and G. B. Field, *Astrophys. J.* **534**, 984 (2000), arXiv:astro-ph/9903384.
 - [14] D. D. Schnack, D. C. Barnes, Z. Mikic, D. S. Harned, and E. J. Caramana, *J. Comput. Phys.* **70**, 330 (1987).
 - [15] F. Ebrahimi, *Ph.D thesis, Nonlinear magnetohydrodynamics of AC helicity injection* (2003).
 - [16] J. B. Taylor, *Physical Review Letters* **33**, 1139 (1974).
 - [17] H. Ji, S. C. Prager, and J. S. Sarff, *Phys. Rev. Lett.* **74**, 2945 (1995).
 - [18] C. D. Cothran, M. R. Brown, T. Gray, M. J. Schaffer, and G. Marklin, *Phys. Rev. Lett.* **103**, 215002 (2009).
 - [19] B. Coppi, J. M. Greene, and J. L. Johnson, *Nuclear Fusion* **6**, 101 (1966).
 - [20] E. Hameiri and A. Bhattacharjee, *Phys. Fluids* **30**, 1743 (1987).
 - [21] F. Ebrahimi, V. V. Mirnov, and S. C. Prager, *Phys. Plasmas* **15**, 055701 (2008).
 - [22] F. Del Sordo, G. Guerrero, and A. Brandenburg, *MNRAS* **429**, 1686 (2013), 1205.3502.
 - [23] D. S. Shapovalov and E. T. Vishniac, *ApJ* **738**, 66 (2011).
 - [24] G. Lesur and G. I. Ogilvie, *Astronomy & Astrophysics* **488**, 451 (2008), 0807.1703.
 - [25] S. W. Davis, J. M. Stone, and M. E. Pessah, *Astrophys. J.* **713**, 52 (2010), 0909.1570.

- [26] J. B. Simon, J. F. Hawley, and K. Beckwith, *Astrophys. J.* **730**, 94 (2011), 1010.0005.